Global Pressure Fields from Scatterometer Winds

JÉRÔME PATOUX

Department of Atmospheric Sciences, University of Washington, Seattle, Washington

RALPH C. FOSTER

Applied Physics Laboratory, Seattle, Washington

ROBERT A. BROWN

Department of Atmospheric Sciences, University of Washington, Seattle, Washington

(Manuscript received 2 July 2002, in final form 23 November 2002)

ABSTRACT

A method is presented for computing global surface pressure fields from satellite scatterometer winds. Pressure gradients are estimated using a two-layer similarity planetary boundary layer model in the midlatitudes and a mixed-layer model in the Tropics. A global pressure field is then fit to the pressure gradients by least squares optimization. A series of surface pressure fields calculated from SeaWinds-on-QuikSCAT (Quick Scatterometer) measurements are compared with numerical weather analyses and buoy measurements. Surface pressure observations in the tropical oceans are scarce and come largely from ships of opportunity. At present no buoy in the Atlantic Ocean and only 10 buoys in the Pacific Ocean have pressure sensors. The method presented here suggests that 0.5°-resolution maps of sea surface pressure can be readily retrieved from available satellite remote sensing data every 12 h in near–real time. It is shown that these fields are at least of comparable quality to the ECMWF analyses.

1. Introduction

Surface pressure fields are traditionally obtained by contouring point measurements of surface pressure (by weather stations, radiosondes, buoys, or ships) or as the gridded output of a numerical weather forecast (NWF) model or data assimilation system. The ability to obtain surface pressure fields from scatterometer data has been demonstrated (Brown and Levy 1986; Harlan and O'Brien 1986; Hsu et al. 1997; Hsu and Liu 1996; Zierden et al. 2000), and the value of the surface pressure field product from satellite scatterometers has been shown in several applications. *Seasat* and the first *European Remote Sensing Satellite* (*ERS-1*) vector winds first demonstrated the shortcomings of numerical analyses in the Tropics and Southern Hemisphere (Levy and Brown 1991; Brown and Zeng 1994). Using surface pressure gradients from buoy data as surface truth for scatterometer wind–derived pressure gradients impetus was furnished to change the scatterometer model function and ''climatology'' to increase winds in the moderate range and add very high winds in storms (Foster and Brown 1994; Brown 1998, 2000; Zeng and Brown 1998, 2001). The use of the surface pressure field as a smoothing product allowed Patoux and Brown (2001) to produce continuous SeaWinds-on-QuikSCAT (QS) wind fields in the midlatitudes (QuikSCAT is the Quick Scatterometer Satellite).

However, these methods have been inherently limited to the midlatitudes and do not resolve the pressure distribution near the equator. For many years, this has been a deterrent to using scatterometer data for computing swath-long (i.e., pole to pole) surface pressure fields. NWF models would likely benefit from real-time swaths of surface pressures for assimilation. General circulation models with mesoscale resolution will benefit from assimilating the scatterometer winds (Conaty et al. 2001), as well as from the mesoscale structure present in the corresponding surface pressure fields. The current coverage of QuikSCAT ensures an almost global picture of the surface winds over the ocean roughly every 12 hours, with relatively small gaps between the swaths. A scheme that estimates the surface pressure in the Tropics as well as in the midlatitudes would thus provide two quasi-global marine surface pressure fields per day. Moreover, a systematic estimation of surface pressure from scatterometer winds over the tropical ocean would

Corresponding author address: Jérôme Patoux, Department of Atmospheric Sciences, University of Washington, 408 ATG Building, Box 351640, Seattle, WA 98195-1640.
E-mail: jerome@atmos.washington.edu

be an improvement over the sparse pressure observations from isolated buoys, islands, and ships.

In a recent article, Stevens et al. (2002) (hereinafter STV) describe a simple mixed-layer model for the tropical planetary boundary layer (PBL) based on a force balance among pressure gradient force, Coriolis force, surface drag, and entrainment flux of free-tropospheric momentum into the boundary layer. They apply it to a climatological dataset of surface pressures and free-tropospheric winds over the Pacific basin to estimate the climatological surface winds. By matching the estimated surface winds to the climatological values, they derive two optimal parameters for the inclusion of entrainment into the PBL structure. These are the entrainment rate and the boundary layer depth, which are assumed to have constant values over the domain. The resulting model is successful in reproducing the climatological surface wind field.

Here, we apply the inverse of this model to estimate pressure gradients (and subsequently the surface pressure field) from the surface wind field in the Tropics. We then can blend this PBL model with the midlatitude model to provide a continuous global model. The scheme is first described in section 2. The data used to assess the resulting pressure fields are described in section 3. The sensitivity to entrainment rate, boundary layer depth, and upper-level winds is investigated in section 4. The scheme is then assessed with NWF analysis data (section 5a) and with scatterometer and buoy data (section 5b).

2. Methods

The retrieval of a pole-to-pole oceanic surface pressure field is a four-step process: surface pressure gradients are obtained in the midlatitudes with a two-layer similarity PBL model; they are obtained in the Tropics with a mixed-layer model; three pressure fields (Northern Hemisphere, Tropics, Southern Hemisphere) are obtained from the pressure gradient fields by least squares optimization; and the three pressure fields are blended in the overlapping latitudinal bands. The resulting pressure pattern is given an absolute value using one or more pressure observations.

a. The two-layer similarity model

The University of Washington Planetary Boundary Layer (UWPBL) model used to calculate gradient or geostrophic wind vectors from surface wind vectors (the so-called inverse model) has been extensively documented (Brown and Levy 1986; Brown and Liu 1982; Brown and Zeng 1994; Patoux 2000). Because the new element here is the mixed-layer model in the Tropics, the midlatitude solution will be only briefly described. At each point of a scatterometer swath or numerical model grid for which a surface wind vector is available, the PBL wind profile is approximated by patching a modified Ekman spiral to a logarithmic surface layer. Stratification and baroclinicity (Foster et al. 1999; Foster and Levy 1998) are taken into account by including surface air temperature, sea surface temperature, and relative humidity, where available (typically, gridded fields from an NWF analysis). Secondary flows are parameterized (Brown 1970, 1981). The gradient wind vector is thus estimated and the corresponding geostrophic wind vector and pressure gradient are calculated using the gradient wind correction described in Patoux and Brown (2002).

b. The mixed-layer model

As we approach the equator, the Coriolis force decreases and the midlatitude model fails to approximate the boundary layer dynamics correctly, primarily because of its assumption of Ekman layer dynamics and lack of entrainment processes. The Ekman depth becomes infinite, and the modified Ekman spiral model is not valid. Here we construct a model for the Tropics built from the simple mixed-layer model described by STV.

STV integrate the steady-state balance equations over the depth h of the boundary layer (momentum integral):

$$f\mathbf{k} \times \mathbf{U} + \frac{1}{\rho_0}\nabla P = \frac{\boldsymbol{\tau}(h) - \boldsymbol{\tau}(0)}{h}, \tag{1}$$

where $\mathbf{U} = (U, V)$ and P are the bulk wind and bulk pressure, respectively,

$$\mathbf{U} = \frac{1}{h}\int_0^h \overline{\mathbf{u}}\, dz \quad \text{and} \quad P = \frac{1}{h}\int_0^h \overline{p}\, dz, \tag{2}$$

and $\boldsymbol{\tau}(0)$ and $\boldsymbol{\tau}(h)$ are the turbulent stresses at the bottom and top of the boundary layer (boldface indicates vectors). We express the surface stress as

$$\boldsymbol{\tau}(0) = u_*^2 \frac{\overline{\mathbf{u}_{10}}}{|\overline{\mathbf{u}_{10}}|}, \tag{3}$$

where u_* is the friction velocity and $\overline{\mathbf{u}_{10}} = (u_{10}, v_{10})$ is the neutral-equivalent 10-m surface wind vector. STV emphasize the critical importance of entrainment at the top of the boundary layer. The relative importance of momentum entrainment is less in the midlatitudes, but it is a first-order effect in the Tropics. STV parameterize the entrainment flux as

$$\boldsymbol{\tau}(h) = w_e \Delta\mathbf{U} = w_e(\mathbf{U}_T - \mathbf{U}), \tag{4}$$

where $\mathbf{U}_T = (U_T, V_T)$ is the wind above the boundary layer and w_e is an entrainment velocity. Mean values of w_e and h are chosen so as to minimize the error when calculating the surface wind climatological values from analyzed pressure fields and free tropospheric winds (on a 1° grid). They found a boundary layer depth h of 300–500 m and an entrainment velocity w_e of 0.88–1.00 cm s^{-1} as optimal parameters.

Here we adopt a similar scheme, except that we know the surface wind vector (scatterometer wind), impose a climatological free-tropospheric wind, and endeavor to estimate the pressure gradient. The wind profile is found by integrating

$$\frac{d}{dz}\left(K\frac{d\overline{u}}{dz}\right) = \frac{1}{\rho_0}\left(\frac{\partial p}{\partial x}\right) - f\overline{v}, \tag{5a}$$

$$\frac{d}{dz}\left(K\frac{d\overline{v}}{dz}\right) = \frac{1}{\rho_0}\left(\frac{\partial p}{\partial y}\right) - f\overline{u}, \quad \text{and} \tag{5b}$$

$$K = \frac{ku_*h}{\phi_m(\zeta)}\left[\frac{z}{h}\left(1 - \frac{z}{h}\right)^2\right], \tag{5c}$$

using a classical fourth-order Runge–Kutta method (Press et al. 1992). The form of K is based on the K-profile PBL model of Troen and Mahrt (1986). The surface layer stratification parameter is $\zeta = z/L$, and L is the Obukhov length; $\phi_m(\zeta)$ is the Monin–Obukhov stratification correction for momentum. Because we are primarily interested in retrieving surface pressure in the Tropics from scatterometer winds alone, the K profiles assume neutral stratification, that is, $\phi_m(\zeta) = 1$. Additional inputs would be needed to calculate the stratification.

We make a first guess on the pressure gradient, which we assume to be constant throughout the boundary layer, and obtain a first wind profile. The bulk wind is calculated by integration of this profile, and a new estimate of the pressure gradient is obtained from the bulk force balance (1):

$$\frac{P_x}{\rho} = fV - \frac{w_e}{h}(U_T - U) + \frac{u_*^2}{h}\frac{u_{10}}{|\overline{\mathbf{u}_{10}}|} \quad \text{and} \tag{6a}$$

$$\frac{P_y}{\rho} = -fU - \frac{w_e}{h}(V_T - V) + \frac{u_*^2}{h}\frac{v_{10}}{|\overline{\mathbf{u}_{10}}|}, \tag{6b}$$

where $h = 500$ m and $w_e = 1$ cm s^{-1}. A final value for the pressure gradient is obtained by convergence within a few iterations.

The method is verified to be qualitatively consistent with both STV's example profiles in the Tropics and the geostrophic winds obtained with the UWPBL inverse model when applied to the midlatitudes where entrainment is less important. Note that the values for h and w_e obtained by STV are climatological means, but they are used here to solve ''individual'' cases. In a similar way, climatological free-tropospheric winds (mean monthly winds on a 2.5° grid) are used to calculate ''instantaneous'' wind profiles on a 0.5° grid. The results are expected to depart from the values one would obtain if the entrainment were known. Our experiments and sensitivity tests (below) suggest, however, that useful tropical pressure fields are obtained using these climatological data to define the upper boundary condition on the PBL solution.

c. The pressure field retrieval

These two models yield three sets of zonal (p_λ) and meridional (p_ϕ) pressure gradients—two in the midlatitudes (UWPBL from 60° to 10°S and from 10° to 60°N) and one in the Tropics (mixed-layer model from 20°S to 20°N). At each point of the corresponding grids, we can write, in matrix notation (Brown and Zeng 1994),

$$\mathbf{Hx} = \mathbf{y}$$

where

$$\mathbf{H} = \begin{vmatrix} \dfrac{1}{a\cos\phi}\dfrac{\partial}{\partial\lambda} \\ \dfrac{1}{a}\dfrac{\partial}{\partial\phi}, \end{vmatrix} \qquad \mathbf{x} \equiv P, \quad \text{and} \quad \mathbf{y} \equiv \begin{vmatrix} P_\lambda \\ P_\phi, \end{vmatrix} \tag{7}$$

where a is the radius of the earth, λ is the longitude, and ϕ the latitude. We can then find an approximate solution for $\mathbf{x}$ by a least squares optimization scheme:

$$|\mathbf{H}^T\mathbf{Hx} - \mathbf{H}^T\mathbf{y}|^2 \equiv 0. \tag{8}$$

The solution matrix $\mathbf{x}$ defines a grid of zero-mean relative pressure values. Absolute values of pressure can be obtained by a second least squares fit to pressure observations, such as buoy measurements. The pressures can also be smoothed and corrected for erroneous scatterometer wind vectors or contamination by rain as described in Patoux and Brown (2001).

The three resulting pressure fields are blended as described in the appendix.

3. Data

The SeaWinds-on-QuikSCAT level-2B surface wind vectors were used, discarding the vectors flagged for rain contamination (Wentz and Smith 1998). The wind vectors are interpolated onto the 0.5° grid on which the UWPBL model is run.

In section 5, buoy pressure differences obtained from the National Oceanic and Atmospheric Administration (NOAA) National Data Buoy Center (NDBC) archives and from the NOAA Tropical Atmosphere–Ocean (TAO) Array project are compared with the UWPBL bulk pressure gradients. UWPBL surface pressure fields (50-km resolution) are also compared with global pressure analyses at synoptic times obtained from the European Centre for Medium-Range Weather Forecasts (ECMWF) (1.25° × 1.12° grid).

Mean monthly 925-hPa winds obtained from the NOAA Climate Diagnostics Center were used to estimate the free-tropospheric winds in the Tropics. The height of the 925-hPa level is about 650–700 m, which is close to the top of the boundary layer determined as the optimal fit by STV (i.e., 500 m). They used 850-hPa winds as a proxy to the winds above the PBL to minimize the effects of the boundary layer scheme on the analyzed winds, even though the 850-hPa surface

is about 1300–1400 m. Here, we performed all of our calculations with both 925- and 850-hPa winds and found that better results were obtained with 925-hPa analyzed winds. The wind vectors are available on a 2.5° grid and are interpolated onto our 0.5° grid. Twelve monthly mean values are calculated at each grid point based on 1948–2002.

We present in sections 4 and 5 a detailed analysis of the method. To demonstrate the model we show here a randomly selected example of a swath-long pressure field retrieved with the method described in section 2. It is shown in Fig. 1 where it is compared with the corresponding ECMWF analysis from 30 min later. Absolute values of pressure were determined by least squares fitting of the UWPBL field to ECMWF. Good agreement can be observed throughout the swath in the positioning and intensity of the two low pressure systems in the midlatitudes and in the positioning of the 1012-hPa contours around 10°N and 10°S. The weak high pressure region appearing at 30°S does not appear in the QS-derived field. A large number of pressure fields were similarly created and checked for visual consistency, and they revealed similar agreement with the corresponding ECMWF analyses. A more detailed analysis of the method follows.

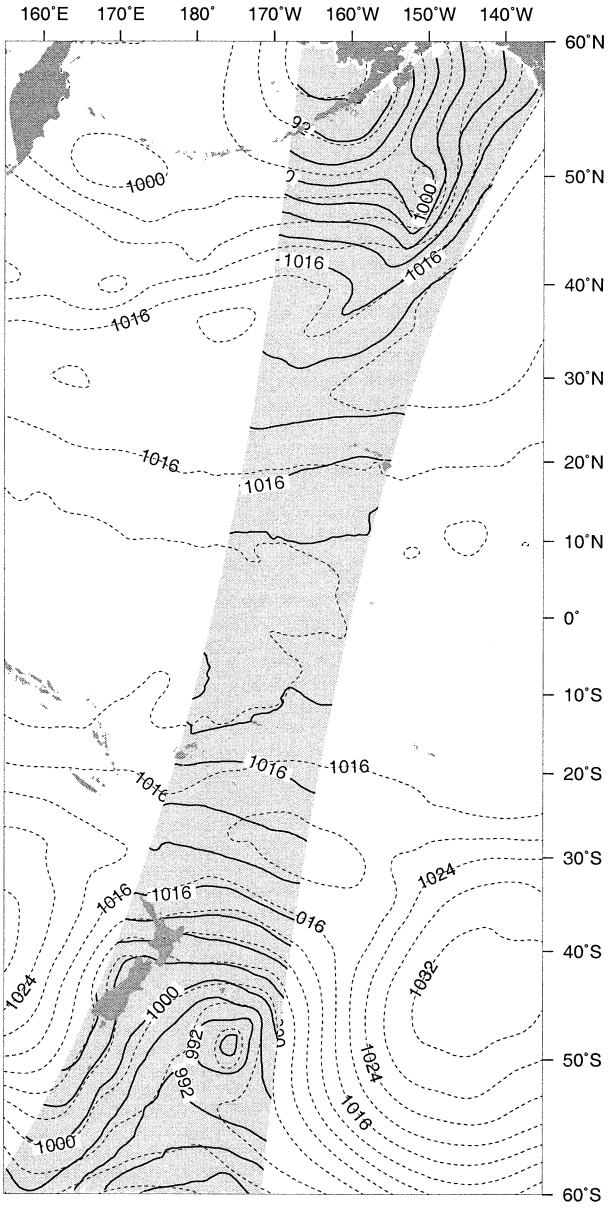

FIG. 1. Comparison between the final pressure field calculated from QS data at 0530 UTC (solid lines) and the corresponding ECMWF pressure field at 0600 UTC (dashed lines), on 20 Sep 1999. Labels appearing inside (outside) the swath refer to the QS-derived (ECMWF derived) contours.

4. Sensitivity to optimal parameters

The pressure fields are derived from thousands of individual scatterometer wind vectors. It has been shown that scatterometer wind errors can be modeled by independent normally distributed errors in each component (Freilich and Dunbar 1999). Hence, the error in pressure retrieval attributable to wind error alone should not lead to systematic error in the pressures because a least squares pressure retrieval will tend to distribute the error throughout the field. However, systematic error could be introduced by biases in the PBL model used to estimate pressure gradients from the winds. Patoux and Brown (2002) showed that using gradient wind vectors instead of geostrophic wind vectors to retrieve pressure fields could introduce biases of up to 20% in synoptic pressure differences. In a similar way, asymmetry in the thermal advection regime can introduce large biases in midlatitude pressure retrievals (Foster and Levy 1998; Foster et al. 1999). Hence, we assess the likelihood of systematic biases in the tropical pressure retrieval model.

For the tropical part of the model, entrainment is recognized to be a first-order effect, and, because it is parameterized, it is important to evaluate the impact of the two parameters, the entrainment velocity w_e and the boundary layer depth h, as well as the assumed upper-level wind field. This is achieved by choosing a typical situation in which the free-tropospheric wind is purely zonal and easterly ($U_T = -6$ m s^{-1}) and the surface wind is easterly with a small northerly component ($u_{10} = -5$ m s^{-1}, $v_{10} = -1$ m s^{-1}). The corresponding pressure gradients are calculated for different values of h (300–1000 m) and w_e (0.2–2.0 cm s^{-1}). The results are shown in Fig. 2.

Figures 2a,c show that shallower boundary layers are more sensitive to changes in the entrainment velocity than are deeper boundary layers. For a given PBL depth, increasing w_e enhances the meridional pressure gradient and reduces the zonal pressure gradient. In this case, free-tropospheric momentum is rapidly mixed into the PBL and affects the whole wind profile (it resists the turning of the wind) and thus the bulk force balance.

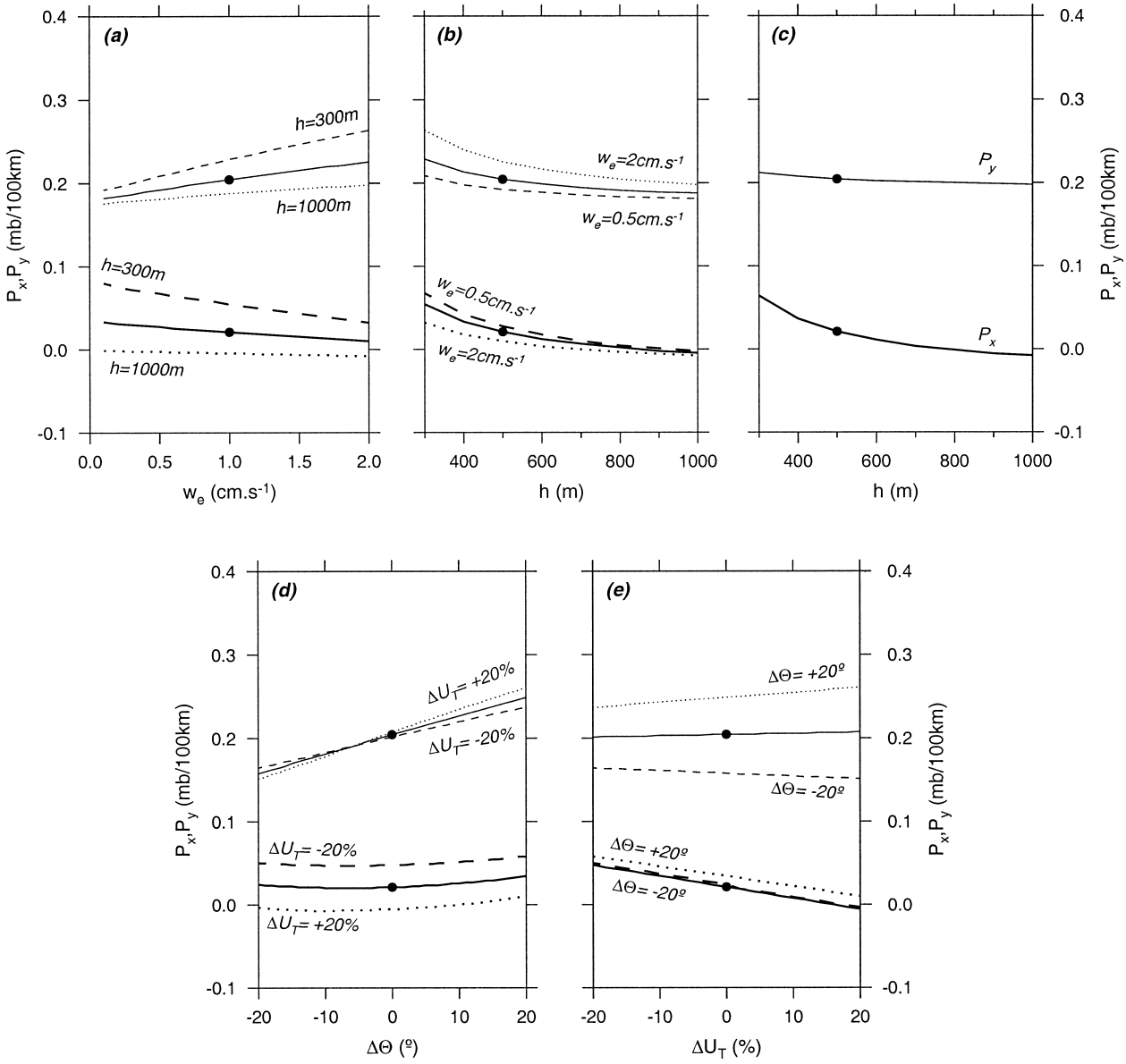

FIG. 2. Sensitivity of (top) meridional (thin lines) and (bottom) zonal (thick lines) pressure gradient calculations to (a) w_e for h = 300, 500, and 1000 m; (b) h for w_e = 0.5, 1, and 2 cm s^{-1}; (c) h with the ratio w_e/h kept constant (=2 × 10^{-5} s^{-1}); (d) changes in free-tropospheric wind direction for −20%, 0, and +20% changes in wind speed; and (e) changes in free-tropospheric wind speed for −20°, 0, and +20° changes in wind direction. The dots indicate the parameters used in the current analyses.

Deeper boundary layers with small entrainment velocities are not very sensitive to changes in w_e or h (i.e., the curves flatten out in Figs. 2a,b). The maximum change in P_x and P_y encountered when one parameter takes on the whole range of values while the other parameter is held constant, is about 0.1 hPa (100 km)$^{-1}$. A more realistic range of values is one in which h changes by 200 or 300 m and w_e changes by 0.5 cm s^{-1}. In this case, the maximum change in P_x and P_y is on the order of 0.02–0.03 hPa (100 km)$^{-1}$.

Figure 2c shows the sensitivity to h when the ratio w_e/h is held constant at 2 × 10^{-5} s^{-1}. It is almost zero for P_y and is somewhat larger for P_x in shallower boundary layers. Intuition for this behavior can be gained by looking at (6). Because the surface drag is mostly zonal (v_{10} small), P_y is determined essentially by the meridional component of $\mathbf{U}_T - \mathbf{U}$, which is a factor of w_e/h. Because w_e/h is held constant in Fig. 2c, P_y is not expected to vary much. However, P_x should be more sensitive in a shallow boundary layer. If w_e/h is held constant, the entrainment flux term in (6a) is constant. However, the surface drag contribution scales as $1/h$, so increasing h decreases P_x. As a result, P_y is less sensitive to changes in h than P_x, and the real uncertainty on the

retrieved pressure gradients is less than the 0.02–0.03 hPa (100 km)$^{-1}$ indicated above. This number can be used as a worse-case estimate of the error.

The sensitivity to the free-tropospheric wind vector was investigated by rotating $\mathbf{U}_T$ by $\pm 20°$ and by varying its speed by $\pm 20\%$. The results are shown in Fig. 2d,e. The range of values taken by P_x and P_y is similar to that obtained in the previous sensitivity analysis, but the sensitivity of P_y to changes in the wind direction is high for all wind speeds. By rotating the upper boundary condition, we effectively rotate the whole force balance, which in turn significantly affects the integrated wind profile. Note, moreover, that a $\pm 20°$ error on the direction of $\mathbf{U}_T$ is not necessarily an upper bound to the range of errors likely to occur, especially when we are using the climatological free-tropospheric winds to force the model. Larger directional errors were actually observed in the analyses presented in section 5b when comparing the climatological winds with the closest-in-time ECMWF-analyzed winds. The quantitative comparisons also suggest that the pressure retrieval can be sensitive to the choice of free-tropospheric winds at individual points. However, these small-scale effects are minimized by the least squares optimization, and, as shown below, acceptable pressure retrievals can be obtained using the climatological winds.

The same sensitivity analysis has been performed on various wind geometries representative of the Tropics, with similar results and uncertainties on the pressure differences of interest in a scatterometer swath.

5. Results

a. Assessment of the global model with NWF data

The combined UWPBL–mixed-layer model, now referred to as the UWPBL global model, is first assessed by comparing ECMWF analysis surface pressure fields with the pressure fields retrieved with the described method applied to ECMWF analysis surface winds. An example of such a comparison is shown in Fig. 3 for 1200 UTC 28 July 1999, where the solid lines are UWPBL isobars and the dashed lines are ECMWF isobars (4-hPa interval). It reveals a fairly typical synoptic situation, with a depression north of the Aleutian Islands (the ''Aleutian low'') and an anticyclone occupying much of the North Pacific Ocean (the ''Hawaiian high''). In the southern Pacific Ocean, the situation is reversed, with an anticyclone around 55°S and a cyclone around 40°S. Along the trough extending northwest from the edge of that storm one notes two smaller depressions. In the Tropics there are two low pressure regions at 140°E and 160°W. The two pressure fields agree well visually, and quantitatively, with a root-mean-square (rms) difference of 1.7 hPa.

Because the skill of the UWPBL model in the midlatitudes has been previously demonstrated, the emphasis here is on the tropical region, shown in Fig. 4. It contrasts the ECMWF pressure field (Fig. 4a, same as dashed lines in Fig. 3) with the surface pressure field calculated with the UWPBL global model from the ECMWF surface wind vectors and mean monthly 925-hPa winds (Fig. 4b, same as solid lines in Fig. 3). Figure 4c shows the surface pressure field calculated with the UWPBL model and the analyzed 925-hPa wind vectors. Because the pressure gradients are much weaker than in the midlatitudes, the isobars are plotted at 2-hPa intervals. Each pressure field contains overall the same features (a depression at 160°W; a larger low pressure region northeast of Indonesia; a fairly uniform increase in pressure to the north; and, to the south, a trough of low pressures at 170°E separating two ridges of higher pressures), but Figs. 4a and 4c agree better in the positioning, extent, and intensity of those features. This result is confirmed by calculating the rms difference between Figs. 4a and 4b (1.6 hPa) and between Figs. 4a and 4c (1.4 hPa). This is consistent with the idea that using the actual free-tropospheric winds would lead to an improvement when compared with climatological winds. In this particular case, we verified that the 925-hPa winds did not depart significantly from the mean monthly July winds. In other cases for which the 925-hPa winds differ greatly from the climatological winds, the improvement is larger.

To obtain a better quantitative estimate and because the pressure distribution in the Tropics is relatively ''flat'' and it is thus difficult to estimate visually the degree to which the pressure fields agree, 30 pressure fields were calculated, along with the average standard deviation from the ECMWF pressures. The standard deviation is 1.1 hPa in the midlatitudes (for pressure variations on the order of 10–15 hPa), 2.2 hPa in the Tropics when using the climatological values of 925-hPa winds, and 1.2 hPa when using the analyzed 925-hPa winds (for pressure variations on the order of 2–3 hPa). This result shows that the level of compatibility between the UWPBL global model and the ECMWF NWF model is high in the midlatitudes and is fairly good in the Tropics. This comparison alone does not point to the superiority of one model over the other, nor does it enable us to quantify the skill of the UWPBL global model in estimating ''real'' pressure gradients.

b. Assessment of the global model with buoy measurements

Our best tool for assessing the global model is a comparison with actual measurements of surface pressure over the ocean. However, such measurements by buoys, ships, and weather stations on islands are scarce in the Tropics. The Pilot Research Moored Array in the Tropical Atlantic (PIRATA) buoys cover a substantial area of the tropical Atlantic but do not report surface pressure. The TAO buoys similarly cover a substantial area of the tropical Pacific, but surface pressure sensors are only present on a limited

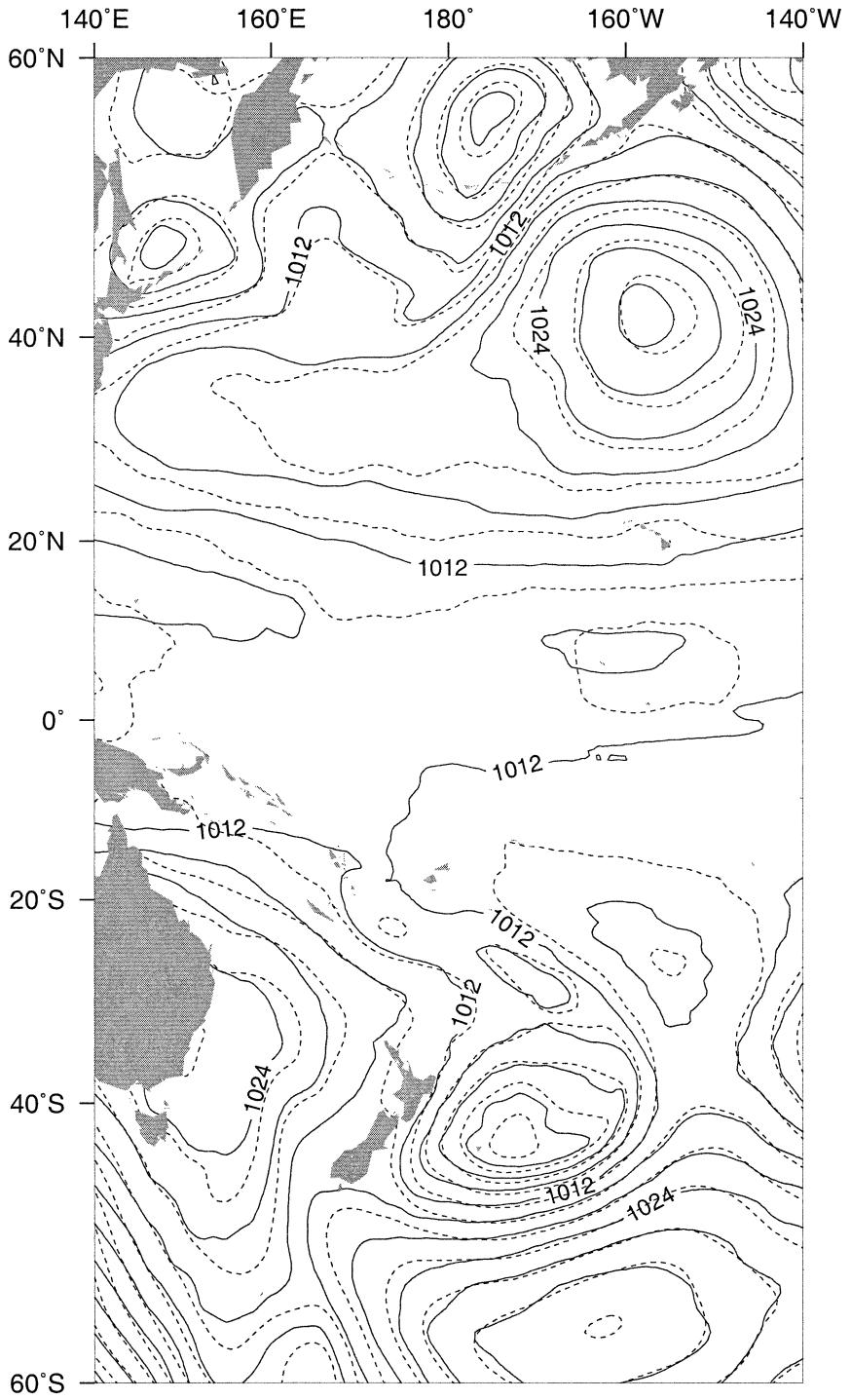

FIG. 3. Comparison between the UWPBL (solid lines) and ECMWF (dashed lines) pressure fields.

number of buoys along the 95° and 110°W longitude lines. We use here a collection of NDBC and TAO buoys in the eastern Pacific Ocean, shown in Fig. 5. The time range of available measurements from the TAO buoys is limited to about a year at 95°W (November 2000–November 2001). The number of times a QS swath intersects the buoy array is also limited. The same configuration is obtained at a recurrent period of 4 days, but the swath shifts slightly eastward over time and the optimal geometry is lost. For these

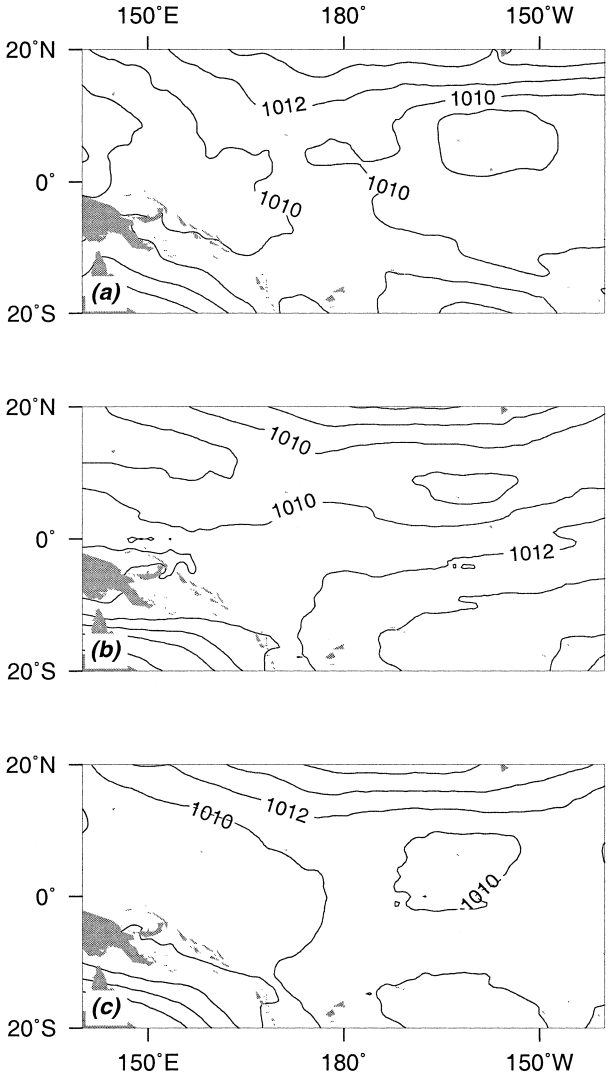

FIG. 4. Comparison among three surface pressure fields on 28 Jul 1999 at 1200 UTC: (a) ECMWF, (b) UWPBL with climatological 925-hPa winds, and (c) UWPBL with ECMWF 925-hPa winds.

reasons, there were 23 cases as shown in Fig. 5a, only 7 cases as in Fig. 5b, and 26 cases as in Fig. 5c.

The problem of assessing our bulk pressure gradient estimates over the eastern tropical Pacific Ocean is made even more difficult by the fact that the pressure gradients are generally weak in that region. Figure 6a shows the monthly mean sea level pressure for the month of June (from the NOAA Climate Diagnostics Center), with the black triangles representing the buoys used in section 1 below. Pressure differences of 2 or 3 hPa can be expected between these two buoys. Weaker pressure gradients can be expected in the zonal direction, as shown in Fig. 6b [with triangles representing buoys used in section 5b(2) below]. An accurate calibration of our model would certainly benefit from other buoy measurements in regions of the tropical ocean where pressure gradients are more pronounced (e.g., around the date line). Note that if this points to the limitations of the present analysis, it also points to the crucial need for pressure measurements in the Tropics. The scatterometer-derived pressure fields could be a good alternative to buoy measurements.

1) MERIDIONAL PRESSURE DIFFERENCES IN THE TROPICS

The pressure difference between the 8°S, 95°W and the 8°N, 95°W TAO buoys (at 0100 UTC) was compared with the pressure difference obtained by running the UWPBL global model with QS surface winds when the QS swath would intersect the buoys as described in Fig. 5a (at 0040 UTC). The results for the 23 different days are recorded in Table 1. On each day, the buoy-measured pressure difference is indicated first, followed by three sets of two values. Each set contains a modeled pressure difference (respectively, UWPBL with climatological 925-hPa winds, UWPBL with 925-hPa analyzed winds, and ECMWF analysis at 0000 UTC) and the difference between that modeled value and the buoy-measured value. The rms averages are indicated in the last row of the table.

Two features should be emphasized. First, the UWPBL-modeled pressure gradient consistently has the right sign, with a tendency to overestimate the pressure difference. Second, the rms error in the global model estimates is 1.2 hPa, which is not negligible when compared with the rms error of 2.3 hPa of the measured quantity. The rms error drops to 0.9 hPa when using analyzed 925-hPa winds. Note that the ECMWF rms error is smaller (0.6 hPa), despite the larger time difference. It should be noted that the TAO buoy measurements are assimilated into the ECMWF analyses.

We investigated the possibility that the tendency to overestimate the pressure differences (i.e., bulk P_y) might be due to a bias in the model, in particular, in the choice of free parameters, as discussed in section 4. The 23 cases considered here cover a 3-month period from the end of April to the end of July, during which the inter tropical convergence zone (ITCZ) is located roughly around 5°N. The flow between the two buoys thus encompasses a large band of southeasterly trade winds (south of the ITCZ), the ITCZ itself, and a few northeasterly trade winds (north of the ITCZ). A visual inspection of the wind fields reveals that the trade winds are fairly consistent over the 3-month period but that the ITCZ region is characterized by numerous convective cells in which the wind variability is high and scatterometer wind vectors are occasionally missing because of rain contamination. If the overestimation of P_y should be assigned to a bias in the model, it would have to be sought in the southeasterly trade wind region. Inspection of the sensitivity analysis results suggests that reducing the entrainment velocity w_e or increasing the PBL depth h would help in overcoming this bias. However, considering the constraining limitations of the analyses, this

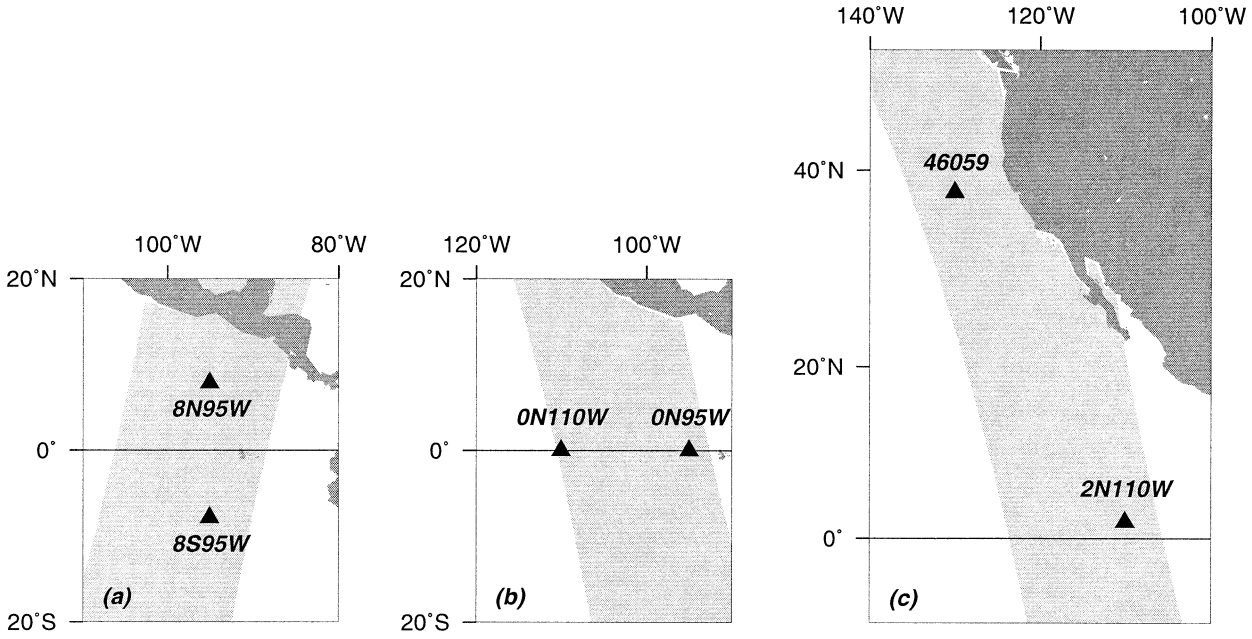

FIG. 5. Buoy and QS-swath geometry used to compare modeled and measured pressure differences: (a) meridional pressure differences in the Tropics, (b) zonal pressure differences in the Tropics, and (c) meridional pressure differences from the Tropics to the midlatitudes.

is only proposed as a possible subject for future investigation.

2) ZONAL PRESSURE DIFFERENCES IN THE TROPICS

The same analysis as above was performed using two TAO buoys separated by about 1600 km at the same latitude (see Fig. 5b). The results are presented in Table 2, with the same format as Table 1 for comparison. The values are valid at 1300 (TAO), 1240 (QS), and 1200 UTC (ECMWF) on each day.

The pressure gradients calculated with the UWPBL global model all have the right sign. In the zonal direction, there is a tendency to underestimate the gradients with the climatological values. That same trend is noticeable in the ECMWF pressure differences but not in the UWPBL with analyzed winds. The rms values are indicated in the last row of the table. The UWPBL rms errors, 0.5 and 0.4 hPa out of 1.1 hPa, are comparable to the meridional error of the previous section. The ECMWF rms error is larger.

At that time of the year (October), and as verified by inspecting the seven corresponding wind fields, the distance separating the two buoys encompasses essentially southerly winds, with a small southeasterly component. The ITCZ is located at 8°N and should not directly affect the bulk pressure gradients calculated along the equator. However, the equatorial region is also characterized by significantly lower wind speeds (below 6 m s^{-1}, as opposed to 8–12 m s^{-1} around 5°S and 5°N). This situation is thought to be due to a change in stratification over the equatorial cold tongue. Because the PBL is more stably stratified, the turbulent flux of momentum is decreased, resulting in lower surface winds (Hayes et al. 1989; Chelton et al. 2001). The UWPBL rms error might be due to the assumption of a neutral PBL. The higher ECMWF rms error might be due to a limitation of the ECMWF PBL model in light-wind conditions as much

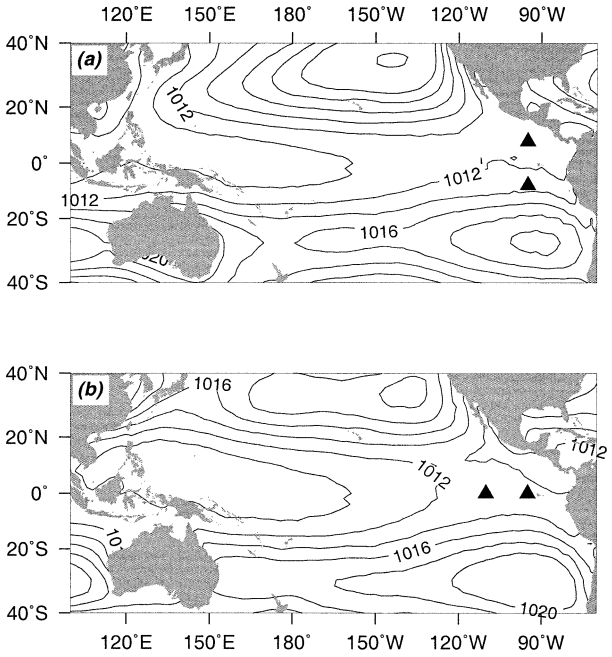

FIG. 6. Mean monthly sea level pressure for the months of (a) Jun and (b) Oct (2-hPa contour intervals, based on Climate Diagnostics Center analyses). The black triangles represent the buoys used in our comparisons.

TABLE 1. Comparison between 1) TAO-measured (8°S, 95°W − 8°N, 95°W) pressure differences (column 2) and UWPBL-with-climatological-winds (column 3), UWPBL-with-analyzed-winds (column 4); and ECMWF (column 5) pressure differences. The errors (columns 4, 6, and 8) are indicated for reference.

Date	Buoys measured	UWPBL (925-hPa climatological winds)		UWPBL (925-hPa analyzed winds)		ECMWF	
		Calc	Diff	Calc	Diff	Calc	Diff
25 Apr 2001	0.3	0.5	+0.2	0.7	+0.4	0.7	+0.4
29 Apr 2001	2.2	0.6	−1.6	1.1	−1.1	1.4	−0.8
3 May 2001	1.3	2.1	+0.8	1.8	+0.5	2.3	+1.0
7 May 2001	1.0	1.8	+0.8	1.3	+0.3	0.5	−0.5
11 May 2001	1.5	1.8	+0.3	1.9	+0.4	1.0	−0.5
15 May 2001	2.4	2.6	+0.2	1.8	−0.6	2.2	−0.2
19 May 2001	1.6	3.0	+1.4	2.2	+0.6	1.3	−0.3
23 May 2001	2.1	4.1	+2.0	2.7	+0.6	3.2	+1.1
31 May 2001	2.9	2.6	−0.3	1.6	−1.3	2.7	−0.2
4 Jun 2001	2.8	4.5	+1.7	3.3	+0.5	2.7	−0.1
8 Jun 2001	3.7	2.6	−1.1	2.1	−1.6	2.9	−0.8
12 Jun 2001	2.3	2.5	+0.2	2.8	+0.5	2.2	−0.1
16 Jun 2001	1.6	1.8	+0.2	2.0	+0.4	1.9	+0.3
19 Jun 2001	2.4	1.6	−0.8	1.3	−1.1	2.4	0.0
23 Jun 2001	2.2	1.9	−0.3	1.3	−0.9	3.2	+1.0
27 Jun 2001	2.5	2.7	+0.2	2.1	−0.4	2.9	+0.4
1 Jul 2001	2.3	3.6	+1.3	2.6	+0.3	2.9	+0.1
5 Jul 2001	3.5	1.9	−1.6	2.0	−1.5	3.2	−0.3
13 Jul 2001	2.7	3.7	+.1.0	3.0	+0.3	2.6	−0.1
17 Jul 2001	2.5	1.8	−0.7	1.3	−1.2	2.8	+0.3
21 Jul 2001	1.9	3.7	+1.8	3.0	+1.1	3.3	+1.4
25 Jul 2001	1.7	3.9	+2.2	3.7	+2.0	2.5	+0.8
29 Jul 2001	3.0	1.6	−1.4	1.9	−1.1	2.2	−0.8
Rms	2.3	2.7	1.2	2.2	0.9	2.4	0.6

as to an inadequate entrainment parameterization or to a statistical artifact. With only seven cases, we are currently unable to address this question. Such cases will, however, be good candidates for refining the model when additional data become available.

3) MERIDIONAL PRESSURE DIFFERENCES BETWEEN THE MIDLATITUDES AND THE TROPICS

Because the pressure gradients are weak in the Tropics, they are not much larger than the uncertainties in the data and the models, which makes the assessment of the global model difficult. The same analysis as before was thus performed on a larger distance (4500 km), covering part of the Tropics and part of the midlatitudes, as shown in Fig. 5c. The results are presented in Table 3 and characterize the skill of the combined two-layer similarity/mixed-layer model in retrieving correct pressure differences. Note that when the measured pressure difference is negative (column 2), the numbers in columns 4, 6, and 8 are positive (negative) if the model overestimates (underestimates) the pressure gradient, independent of the sign. This emphasizes better the tendency of the model to produce tighter or weaker pressure gradients.

With the exception of two singular cases in which the pressure difference between the two buoys was 0.5 and 0.9 hPa, the pressure differences calculated with the global model had consistently the same sign as the measured value, with a tendency to underestimate it, whereas ECMWF has a tendency to overestimate it. The UWPBL-with-climatological-winds rms error is 1.9 hPa

TABLE 2. Same as Table 1; but for 0°, 110°W − 0°, 95°W TAO buoys.

Date	Buoys Measured	UWPBL (925-hPa climatological winds)		UWPBL (925-hPa analyzed winds)		ECMWF	
		Calc	Diff	Calc	Diff	Calc	Diff
5 Oct 2001	0.7	1.3	+0.6	0.8	+0.1	0.0	−0.7
9 Oct 2001	0.6	0.2	−0.4	0.7	+0.1	−0.7	−1.3
13 Oct 2001	0.5	0.1	−0.4	0.8	+0.3	0.1	−0.4
17 Oct 2001	1.5	0.9	−0.6	1.3	−0.2	0.6	−0.9
21 Oct 2001	1.3	1.3	0	1.8	+0.5	0.2	−1.1
25 Oct 2001	1.6	1.0	−0.6	0.7	−0.9	1.5	−0.1
29 Oct 2001	0.7	0.6	−0.1	0.5	−0.2	0.9	0.2
Rms	1.1	0.9	0.5	1.0	0.4	0.8	0.8

TABLE 3. Same as Table 1; but for NDBC 46059 − 2°N, 110°W TAO buoy.

Date	Buoys Measured	UWPBL (925-hPa climatological winds)		UWPBL 925-hPa analyzed winds)		ECMWF	
		Calc	Diff	Calc	Diff	Calc	Diff
12 Apr 2001	15.6	15.6	0.0	14.8	−0.8	17.4	+1.8
16 Apr 2001	−3.4	−3.9	+0.5	−4.9	+1.5	−0.6	−2.8
20 Apr 2001	2.3	2.9	+0.6	3.1	+0.8	4.6	+2.3
24 Apr 2001	15.9	11.8	−4.1	13.0	−2.9	16.9	+1.0
28 Apr 2001	9.6	7.9	−1.7	8.4	−1.2	10.8	+1.2
2 May 2001	21.2	19.9	−1.3	21.5	+0.3	23.5	+2.3
6 May 2001	13.9	12.7	−1.2	13.6	−0.3	15.0	+1.1
10 May 2001	11.8	11.8	0.0	13.1	+1.3	13.3	+1.5
18 May 2001	12.6	10.8	−1.8	12.2	−0.4	14.4	+1.8
22 May 2001	0.5	−1.9	−2.4	−2.4	−2.9	0.3	−0.2
26 May 2001	6.1	4.9	−1.2	4.9	−1.2	7.9	+1.8
30 May 2001	12.7	12.2	−0.4	11.0	−1.7	13.8	+1.1
3 Jun 2001	10.7	9.5	−1.2	10.0	−0.7	12.1	+1.4
7 Jun 2001	11.1	8.7	−2.4	8.8	−2.3	11.6	+0.5
11 Jun 2001	9.1	8.6	−0.5	8.8	−0.3	11.5	+2.4
15 Jun 2001	14.2	13.3	−1.0	14.3	+0.1	15.4	+1.2
19 Jun 2001	12.2	10.1	−2.2	11.2	−1.1	13.1	+0.9
23 Jun 2001	9.6	7.9	−1.7	8.8	−0.8	10.9	+1.3
27 Jun 2001	0.9	−0.6	−1.5	1.1	+0.2	3.2	+2.3
1 Jul 2001	9.7	5.0	−4.6	6.4	−3.3	10.1	+0.4
5 Jul 2001	12.1	11.0	−1.1	11.7	−0.4	12.1	+0.0
9 Jul 2001	7.7	6.4	−1.3	7.0	−0.7	9.4	+1.7
13 Jul 2001	11.7	8.9	−2.8	10.1	−1.6	12.7	+1.0
17 Jul 2001	8.9	7.7	−1.2	7.8	−1.1	9.6	+0.7
21 Jul 2001	8.0	6.7	−1.3	7.7	−0.4	9.5	+1.5
25 Jul 2001	6.4	8.7	+2.4	9.1	+2.7	7.3	+0.9
Rms	11.0	9.8	1.9	10.4	1.5	12.1	1.5

and is larger than the ECMWF rms error (1.5 hPa). The UWPBL-with-analyzed-winds rms error is 1.5 hPa and is comparable to the ECMWF rms error.

The same analysis was performed between NDBC buoys 46001, 46005, and 46006 and the 2°N, 110°W TAO buoy with similar results (not shown here).

6. Discussion

The current results enable us to make the following comments. 1) The momentum-integral PBL model developed by STV can be successfully applied to the retrieval of surface pressure fields from scatterometer winds in the Tropics using STV's values for w_e and h and assuming climatological upper-level winds. 2) The surface pressure fields produced by the new model are similar to those produced by ECMWF. 3) The validity of the model is supported by the fact that using 925-hPa analyzed winds is an improvement over using climatological winds. 4) The bulk pressure gradients obtained with the global model have the correct sign, even for small values on the order of 1–2 hPa, compare well to buoy measurements, and are nearly as accurate as those obtained by ECMWF. It must be emphasized that the global model has no knowledge of the buoy measurements, whereas they are assimilated into ECMWF analyses. 5) Considering the simplicity and the current limitations of the model in the Tropics, further refinements will probably bring even better results. In the meantime, these scatterometer-derived tropical surface pressure fields can provide dense, useful information in this data-poor and climatologically important region.

These comments are supported by systematic comparisons of pressure fields and bulk pressure gradients. The global model and ECMWF are consistent with each other within 1.1 hPa in the midlatitudes, 1.2 hPa in the Tropics when using ECMWF analyzed 925-hPa winds, and 2.2 hPa (in the Tropics), when using climatological 925-hPa winds. The UWPBL-with-climatological-winds/UWPBL-with-analyzed-winds/ECMWF bulk surface pressure gradient rms errors (when compared with buoys) are 1.2/0.9/0.6 hPa, respectively, in the Tropics in the meridional direction, 0.5/0.4/0.8 hPa, respectively, in the Tropics in the zonal direction (based only on seven cases), and 1.9/1.5/1.5 hPa, respectively, on a larger distance covering both the Tropics and midlatitudes. These results are very encouraging, although the data available for verification are limited.

Because the entrainment of free-tropospheric momentum into the PBL is parameterized by a relatively simple expression with two free parameters, w_e and h, and because the model requires a field of free-tropospheric wind vectors above the PBL, the sensitivity to these quantities must be assessed. The sensitivity analysis in section 4 shows that the uncertainty in the w_e and h parameters translates into a typical 0.02–0.03 hPa $(100\ \text{km})^{-1}$ uncertainty on the pressure gradients, this value being smaller if the ratio w_e/h is considered to

remain constant. The model is more sensitive to uncertainties in the free-tropospheric wind field. This is of concern when using climatological data to force the model, because errors can be introduced locally. An operational implementation could easily employ forecast 925-hPa winds to reduce this error.

A series of calculations was also performed with 850-hPa climatological winds and 850-hPa analyzed winds. The comparison of bulk pressure gradients with buoys produced rms errors of (to be compared with errors in the previous paragraph) 2.3/1.4/0.6 hPa, respectively, in the Tropics in the meridional direction; 0.5/0.6/0.8 hPa, respectively, in the Tropics in the zonal direction; and 1.9/1.6/1.5 hPa, respectively, in the Tropics/midlatitudes cases. The results were systematically better (or the same) when using 925-hPa winds. Relative confidence in the choice of parameters is gained through these sensitivity results.

The comparisons of the tropical surface pressure retrieval with buoy data suggest that the retrieved meridional pressure gradients (P_y) are too large. Based on sensitivity analyses, there is a suggestion that decreasing w_e or possibly increasing h would tend to improve the surface pressure retrievals in the Tropics, although increasing h tends to lower the overall sensitivity of the model. However, the TAO buoys with pressure sensors used in this study cover a region in which the wind dynamics are complex. They encompass, in particular, the convective PBL encountered along the ITCZ, where the current implementation of the model is not expected to perform as well. Moreover, decreasing w_e or increasing h will affect the zonal pressure gradient (P_x) retrieval. Although the buoys used in section 5b(2) are far from the ITCZ and its convective wind regime, they lie along the equatorial cold tongue, where stratification plays an important role and only seven cases are available to assess the retrieval of P_x. As a result, there are not sufficient data to tune the parameters more finely than was done by STV. Hence, this issue must be left for the future when sufficient buoy–scatterometer matchups are available.

The model used to estimate the mean flow in the tropical PBL was chosen specifically because of its simplicity and similarity to PBL parameterizations employed in the ECMWF and National Centers for Environmental Prediction (NCEP) analysis/forecasting models. The cubic K profile [(5c)] with or without the so-called nonlocal flux contribution is known to overpredict entrainment severely in convective boundary layers, and fixes have likely been incorporated to improve its performance (e.g., Beljaars and Viterbo 1998). Hence, the ad hoc entrainment flux parameterization employed here, tuned by STV to reproduce tropical surface wind fields from NCEP surface pressures, is adequate for the present.

Important future improvements to the model will include stratification effects in (5c), that is, $\phi_m(\zeta) \neq 1$; a predicted boundary layer height h; extension of the gradient wind correction to the Tropics; and incorporation of nonlocal transport by PBL rolls or other coherent structures. The boundary layer depth is known to vary with the surface stratification (and wind and potential temperature profiles). With the new-era satellites such as the Earth Observing System (EOS) *Terra*/*Aqua* and the future National Polar-Orbiting Operational Environmental Satellite System (NPOESS), it is conceivable that much of the information necessary to estimate the relevant oceanic boundary layer processes may be available from remote sensors. Assessing the model on different regions of the World Ocean and at different times of the year will also produce significant improvements.

It has been shown that including the effects of PBL rolls in the midlatitudes improves the accuracy of PBL parameterizations and pressure retrievals from scatterometers (Brown and Zeng 1994; Brown and Levy 1986). Rolls are known to form in the Tropics. Although the existing roll parameterization (Brown 1981) is invalid in the Tropics, the more general model of Foster (1996) could be incorporated into the framework of the present tropical model, which would allow a single pressure retrieval model to be used in both the Tropics and midlatitudes without patching solutions in the subtropical regions. Because such a unified model could include the dominant PBL processes (variable stratification, entrainment flux, nonlocal fluxes, and thermal wind), it would improve our capability to produce consistent global surface pressure fields from satellite data, including in the data-poor Tropics.

7. Concluding remarks

A simple model for relating surface pressure gradients to surface winds in the Tropics, based on the Stevens et al. (2002) mixed-layer model, is described and incorporated into the UWPBL model to retrieve swath-long (pole to pole) surface pressure fields from scatterometer-measured wind vectors. The pressure gradients are retrieved in the midlatitudes with a two-layer similarity model and in the Tropics by solving a simple force balance among the pressure gradient, Coriolis force, surface drag, and entrainment of free-tropospheric momentum into the PBL. Entrainment is parameterized with an entrainment velocity w_e, a boundary layer depth h, and climatological or analyzed 925-hPa winds. STV's proposed values of 0.01 m s^{-1} and 500 m, respectively, are used throughout this study. The global model is assessed against ECMWF pressure fields and NDBC and TAO buoy bulk pressure gradients.

The prospect of using global pressure fields to initialize NWF models has recently stirred some interest (R. Atlas 2002, personal communication). The UWPBL pressure fields can compete with the ECMWF numerical outputs and have the advantage of containing superior information about the location of surface fronts and low pressure centers, especially in the Southern Hemisphere where measurements are scarce. With an almost com-

plete coverage of the global ocean every 12 h, QS-derived sea level pressure fields and surface-wind fields should prove valuable in NWF model assimilation. Moreover, the 925-hPa winds from the previous analysis, or from the forecast run, could be used to define better the entrainment at the top of the PBL, thus improving the quality of the surface pressure estimates in the Tropics. Current and planned satellite remote sensors may provide sufficient ancillary information to incorporate the effects of stratification and coherent structures into the global model and to improve further the pressure retrievals. In 2003, with the SeaWinds scatterometer on the *Advanced Earth Observing Satellite-II* (*ADEOS-II*) orbiting the earth jointly with the SeaWinds-on-QuikSCAT satellite, a quasi-global picture of the surface winds over the ocean will be available roughly every 6 h, which will improve the resolution of the global pressure fields in both time and space. A refined mixed-layer model in the Tropics will then be extremely valuable.

Acknowledgments. We thank Christopher S. Bretherton for his helpful comments during the research. Authors J. Patoux and R. A. Brown acknowledge support from NASA Grant NS033A-01, administered through Oregon State University, NASA Grant NAG8-1424, and NASA EOS Grant NAGW-2633. Author R. C. Foster acknowledges support from NASA Ocean Vector Winds science team Grant JPL 1216956 and NASA Surface Winds from SAR Grant NAG5-10114.

APPENDIX

Blending Pressure Fields

The inversion is run separately on the Northern Hemisphere [pressure field $p_1(\lambda, \phi)$], the Tropics [$p_2(\lambda, \phi)$], and the Southern Hemisphere [$p_3(\lambda, \phi)$], and the three resulting pressure fields are blended with the following weighting function:

$$p = w_1 p_1 + w_2 p_2 + w_3 p_3, \tag{A1a}$$

$$w_1 = \begin{cases} 1 & \text{if } \phi > 20^\circ\text{N} \\ \dfrac{1}{2}\left\{1 - \cos\left[\dfrac{2\pi(\phi - 10)}{20}\right]\right\} & \text{if } 10^\circ < \phi < 20^\circ\text{N} \\ 0 & \text{if } \phi < 10^\circ\text{N}, \end{cases} \tag{A1b}$$

$$w_2 = \begin{cases} 0 & \text{if } \phi > 20^\circ\text{N} \\ \dfrac{1}{2}\left\{1 + \cos\left[\dfrac{2\pi(\phi - 10)}{20}\right]\right\} & \text{if } 10^\circ < \phi < 20^\circ\text{N} \\ 1 & \text{if } 10^\circ\text{S} < \phi < 10^\circ\text{N} \\ \dfrac{1}{2}\left\{1 + \cos\left[\dfrac{2\pi(\phi + 10)}{20}\right]\right\} & \text{if } 20^\circ < \phi < 10^\circ\text{S} \\ 0 & \text{if } \phi < 20^\circ\text{S}, \end{cases} \tag{A1c}$$

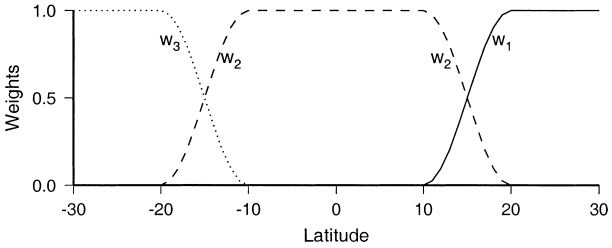

FIG. A1. Weights used in the blending of Northern Hemisphere, tropical, and Southern Hemisphere pressure fields.

$$w_3 = \begin{cases} 0 & \text{if } \phi > 10^\circ\text{S} \\ \dfrac{1}{2}\left\{1 - \cos\left[\dfrac{2\pi(\phi + 10)}{20}\right]\right\} & \text{if } 20^\circ < \phi < 10^\circ\text{S} \\ 1 & \text{if } \phi < 20^\circ\text{S}. \end{cases} \tag{A1d}$$

The value of the weights as a function of latitude are shown in Fig. A1.

The compatibility of the two models was verified by running them independently on the entire swath and verifying their qualitative agreement. Moreover, it can be verified that the inverse model degenerates only smoothly in the overlapping region and becomes inadequate only in the 10°S–10°N latitudinal band. Because the blending is performed in the 10°–20° bands, it does not introduce any major discrepancy.

REFERENCES

Beljaars, A., and P. Viterbo, 1998: Role of the boundary layer in a numerical weather prediction model. *Clear and Cloudy Boundary Layers,* A. Holtslag and P. G. Duynkerke, Eds., Royal Netherlands Academy of Arts and Sciences, 287–403.

Brown, R. A., 1970: A secondary flow model for the planetary boundary layer. *J. Atmos. Sci.,* **27,** 742–757.

——, 1981: Modeling the geostrophic drag coefficient for AIDJEX. *J. Geophys. Res.,* **86,** 1989–1994.

——, 1998: Global high wind deficiency in modeling. *Remote Sensing of the Pacific Ocean by Satellites,* R. A. Brown, Ed., Southwood Press Pty Limited, 69–77.

——, 2000: On satellite scatterometer model functions. *J. Geophys. Res.,* **105,** 29 195–29 205.

——, and W. T. Liu, 1982: An operational large-scale marine planetary boundary layer model. *J. Appl. Meteor.,* **21,** 261–269.

——, and G. Levy, 1986: Ocean surface pressure fields from satellite sensed winds. *Mon. Wea. Rev.,* **114,** 2197–2206.

——, and L. Zeng, 1994: Estimating central pressures of oceanic midlatitude cyclones. *J. Appl. Meteor.,* **33,** 1088–1095.

Chelton, D. B., and Coauthors, 2001: Observations of coupling between surface wind stress and sea surface temperature in the eastern tropical pacific. *J. Climate,* **14,** 1479–1498.

Conaty, A. L., J. C. Jusem, L. Takacs, D. Keyser, and R. Atlas, 2001: The structure and evolution of extratropical cyclones, fronts, jet streams, and the tropopause in the GEOS general circulation model. *Bull. Amer. Meteor. Soc.,* **82,** 1853–1867.

Foster, R. C., 1996: An analytic model for planetary boundary roll vortices. Ph.D. thesis, University of Washington, 195 pp.

——, and R. A. Brown, 1994: On large-scale PBL modelling: Surface wind and latent heat flux comparisons. *Global Atmos.-Ocean Syst.,* **2,** 199–219.

——, and G. Levy, 1998: The contribution of organized roll vortices to the surface wind vector in baroclinic conditions. *J. Atmos. Sci.,* **55,** 1466–1472.

——, R. A. Brown, and A. Enloe, 1999: Baroclinic modifications of midlatitude marine surface wind vectors observed by the NASA scatterometer. *J. Geophys. Res.,* **104,** 31 225–31 237.

Freilich, M. H., and R. S. Dunbar, 1999: The accuracy of the NSCAT 1 vector winds: Comparisons with national data. *J. Geophys. Res.,* **104,** 11 231–11 246.

Harlan, J., Jr. and J. J. O'Brien, 1986: Assimilation of scatterometer winds into surface pressure fields using a variational method. *J. Geophys. Res.,* **91,** 7816–7836.

Hayes, S. P., M. J. McPhaden, and J. M. Wallace, 1989: The influence of sea-surface temperature on surface wind in the eastern equatorial Pacific: Weekly to monthly variability. *J. Climate,* **2,** 1500–1506.

Hsu, C. S., and W. T. Liu, 1996: Wind and pressure fields near tropical cyclone Oliver derived from scatterometer observations. *J. Geophys. Res.,* **101,** 17 021–17 027.

——, M. G. Wurtele, G. F. Cunningham, and P. M. Woiceshyn, 1997: Construction of marine surface pressure fields from scatterometer winds alone. *J. Appl. Meteor.,* **36,** 1249–1261.

Levy, G., and R. A. Brown, 1991: Southern Hemisphere synoptic weather from a satellite scatterometer. *Mon. Wea. Rev.,* **119,** 2803–2813.

Patoux, J., 2000: UWPBL 3.0, The University of Washington Planetary Boundary Layer (UWPBL) Model. Tech. Note, University of Washington, 54 pp.

——, and R. A. Brown, 2001: A scheme for improving scatterometer surface wind fields. *J. Geophys. Res.,* **106,** 23 985–23 994.

——, and ——, 2002: A gradient wind correction for surface pressure fields retrieved from scatterometer winds. *J. Appl. Meteor.,* **41,** 133–143.

Press, W. H., S. A. Teukolsky, W. T. Vetterling, and B. P. Flannery, 1992: *Numerical Recipes in FORTRAN: The Art of Scientific Computing.* Cambridge University Press, 963 pp.

Stevens, B., J. Duan, J. C. McWilliams, M. Münnich, and J. D. Neelin, 2002: Entrainment, Rayleigh friction, and boundary layer winds over the tropical Pacific. *J. Climate,* **15,** 30–44.

Troen, I., and L. Mahrt, 1986: A simple model of the atmospheric boundary layer: Sensitivity to surface evaporation. *Bound.-Layer Meteor.,* **37,** 129–148.

Wentz, F., and D. K. Smith, 1998: Rain effect on NSCAT sigma-0 measurements. *Proc. NSCAT/Quikscat Science Team Meeting,* Kona, HI, Jet Propulsion Laboratory.

Zeng, L., and R. A. Brown, 1998: Scatterometer observations at high wind speeds. *J. Appl. Meteor.,* **37,** 1412–1420.

——, and ——, 2001: Comparison of planetary boundary layer model winds with dropwindsonde observations in tropical cyclones. *J. Appl. Meteor.,* **40,** 1718–1723.

Zierden, D. F., M. A. Bourassa, and J. J. O'Brien, 2000: Cyclone surface pressure fields and frontogenesis from NASA scatterometer (NSCAT) winds. *J. Geophys. Res.,* **105,** 23 967–23 981.